

ORIGINAL ARTICLE

Clinical use of machine learning-based pathomics signature for diagnosis and survival prediction of bladder cancer

Siteng Chen¹ | Liren Jiang² | Xinyi Zheng³ | Jialiang Shao¹ | Tao Wang¹ |
Encheng Zhang¹ | Feng Gao² | Xiang Wang¹  | Junhua Zheng¹

¹Department of Urology, Shanghai General Hospital, Shanghai Jiao Tong University School of Medicine, Shanghai, China

²Department of Pathology, Shanghai General Hospital, Shanghai Jiao Tong University School of Medicine, Shanghai, China

³Department of Pharmacy, Huashan Hospital, Fudan University, Shanghai, China

Correspondence

Junhua Zheng and Xiang Wang, Department of Urology, Shanghai General Hospital, Shanghai Jiao Tong University School of Medicine, No. 100 Haining Road, Shanghai 200080, China.

Emails: zhengjh0471@sina.com (JZ) and seanw_hs@163.com (XW)

Feng Gao, Department of Pathology, Shanghai General Hospital, Shanghai Jiao Tong University School of Medicine, No. 100 Haining Road, Shanghai 200080, China. Email: feng.gao@shgh.cn

Funding information

National Natural Science Foundation of China, Grant/Award Number: 81972393 and 81772705

Abstract

Traditional histopathology performed by pathologists by the naked eye is insufficient for accurate and efficient diagnosis of bladder cancer (BCa). We collected 643 H&E-stained BCa images from Shanghai General Hospital and The Cancer Genome Atlas (TCGA). We constructed and cross-verified automatic diagnosis and prognosis models by performing a machine learning algorithm based on pathomics data. Our study indicated that high diagnostic efficiency of the machine learning-based diagnosis model was observed in patients with BCa, with area under the curve (AUC) values of 96.3%, 89.2%, and 94.1% in the training cohort, test cohort, and external validation cohort, respectively. Our diagnosis model also performed well in distinguishing patients with BCa from patients with glandular cystitis, with an AUC value of 93.4% in the General cohort. Significant differences were found in overall survival in TCGA cohort (hazard ratio (HR) = 2.09, 95% confidence interval (CI): 1.56-2.81, $P < .0001$) and the General cohort (HR = 5.32, 95% CI: 2.95-9.59, $P < .0001$) comparing patients with BCa of high risk vs low risk stratified by risk score, which was proved to be an independent prognostic factor for BCa. The integration nomogram based on our risk score and clinicopathologic characters displayed higher prediction accuracy than current tumor stage/grade systems, with AUC values of 77.7%, 83.8%, and 81.3% for 1-, 3-, and 5-y overall survival prediction of patients with BCa. However, prospective studies are still needed for further verifications.

KEYWORDS

bladder cancer, diagnosis, machine learning, pathomics, prognosis

1 | INTRODUCTION

Bladder cancer (BCa) is the most common malignant tumor of the urinary system, with the fourth incidence among male malignant tumors.¹ In accordance with pathology grading classification, bladder

cancer can be classified into non-invasive urothelial lesions, including urothelial dysplasia and urothelial proliferation of uncertain malignant potential, as well as infiltrating urothelial carcinoma, with divergent differentiations.²

Currently, the accurate clinical diagnosis of BCa mainly depends on histopathology, which is performed by pathologists using medical

Siteng Chen, Liren Jiang, and Xinyi Zheng are equal contributors and co-first authors.

This is an open access article under the terms of the Creative Commons Attribution-NonCommercial License, which permits use, distribution and reproduction in any medium, provided the original work is properly cited and is not used for commercial purposes.

© 2021 The Authors. *Cancer Science* published by John Wiley & Sons Australia, Ltd on behalf of Japanese Cancer Association.

microscopes and by the naked eye. However, some histopathology patterns, such as microcystic urothelial carcinoma and papillary urothelial neoplasm of low malignant potential, could exhibit deceptive appearances.² Traditional immunochemistry methods sometimes could still be insufficient for difficult differential diagnosis. Therefore, an automatically pathological image aiding system could be a convenient and ideal solution.

High-throughput processing of medical images has been widely used to explore mineable high-dimensional data for precision medicine.^{3,4} As a novel technology with highly promising prospects, machine learning is being gradually used in medical image processing for multiple malignant tumors, including breast cancer,⁵ lung adenocarcinoma,⁶ neuro-oncology,⁷ and skin carcinoma.⁸ However, primary use of machine learning technology based on pathology images has not been fully studied for BCa.

Here, using a machine learning algorithm, we constructed and verified automated pathological models for diagnosis and clinical prognosis prediction for patients with BCa.

2 | MATERIALS AND METHODS

2.1 | Patient cohorts

The study included 108 radical or partial cystectomy patients with BCa who received treatment at the Shanghai General Hospital from January 2009 to December 2016 (General cohort). The criteria for selecting these patients were: (a) diagnosed as having primary malignant bladder tumors with relevant clinicopathologic features; (b) being without other tumors diagnosed simultaneously; (c) having access to formalin-fixed and paraffin-embedding (FFPE) BCa samples. Ethical approval for this study was approved by the Research Ethics Committee of Shanghai General Hospital.

Another 406 patients with BCa who met the first 2 inclusion criteria and with access to malignant pathological slice images in The Cancer Genome Atlas (TCGA, <https://portal.gdc.cancer.gov>), were also enrolled for this study (TCGA cohort).

2.2 | Histopathology samples and representative images

All of the 108 FFPE BCa samples were sliced at 5 μm to obtain histological sections that were further stained with hematoxylin (Sigma-Aldrich) and eosin (Sigma-Aldrich). All the H&E-stained slides were carefully reviewed by an experienced pathologist who specialized in genitourinary pathology. A Leica DM2500 LED fluorescence microscope was used to determine the region of interest and select the most representative image from each sample with regards to nuclear pleomorphism, mitosis, carcinoma infiltration, cancer invasion, tumor cell differentiation, and pathological grading. These pathological concerns can be regarded as a typical screenshot of a pathologist following slide diagnosis. Images of 1000 \times 1000 pixels for each

sample were acquired under $\times 400$ magnification. Another 53 normal bladder FFPE samples and 39 glandular cystitis FFPE samples were also obtained from Shanghai General Hospital and processed as mentioned above for further analysis. In TCGA cohort, 406 BCa and 37 normal bladder tissue H&E slice images were processed directly by Leica Aperio ImageScope at $\times 400$ magnification to obtain representative images as mentioned above. Finally, all of the 643 representative images were strictly censored by another independent pathologist for academic rigorously.

2.3 | Extraction of quantitative image features

We built an image processing pipeline (Document S1) for segmentation and feature extraction using multiple modules in CellProfiler.^{9,10} H&E-stained images were firstly unmixed with 1000 \times 1000 pixels via the 'UnmixColors' module. Afterwards, unmixed images were automatically segmented via an 'IdentifyPrimaryObjects' module and an 'IdentifySecondaryObjects' module to identify the cell nuclei and cell cytoplasm. Quantitative image features of object shape, size, texture, and pixel intensity distribution were further extracted via multiple modules, including measure models of 'Object Intensity Distribution', 'Object Intensity', 'Texture', and 'Object Size Shape'. After eliminating unnecessary image features, 345 available quantitative image features (Document S2) were finally selected for further analysis, which were also listed in Table S1.

2.4 | Construction of machine learning-based models for patients with BCa

To construct the machine learning-based diagnosis model for patients with BCa, H&E-stained slice images of 406 BCa and 37 matched normal bladder tissue from TCGA were randomly allocated into 2 independent groups (ratio of 1 to 1) through computer-generated random seed in the R environment, including training cohort and test cohort. In addition, 108 BCa images and 53 normal bladder tissue images from Shanghai General Hospital were grouped as the external validation cohort to verify the validity of the diagnosis model.

Based on 345 available quantitative features of each H&E slice image in the training cohort, the GLMNET package¹¹ was applied to perform least absolute shrinkage and selection operator (LASSO) analysis for selecting BCa-related digital factors and calculating their weighted coefficients to develop a machine learning-based diagnosis model, which was afterwards verified in the test cohort and the external validation cohort, respectively.

The machine learning-based diagnostic score was calculated as follow:

$$\text{Diagnostic score} = \sum_{i=1}^n (C_i \times D_i)$$

where D_i and C_i represent the selected BCa-related image features and the associated weights, respectively.

To construct a clinical prognosis model for patients with BCa, we constructed a LASSO-Cox hazard model¹² based on digital pathological images of 406 patients with BCa in the TCGA cohort (training cohort) to identify survival-related image features. We further created a machine learning-based risk score to increase the flexibility of the prognosis model, which was calculated as follows:

$$\text{Machine learning based risk score} = \sum_{i=1}^n (C_i \times R_i)$$

where R_i and C_i represent the selected survival-related image features and the associated weights, respectively. We next verified our prognosis model in the General cohort (test cohort) and constructed an integrated nomogram in accordance with clinicopathologic factors and risk score, which was further evaluated by calibration with a bootstrapping plot.

2.5 | Statistical analysis

In this study, a comparison of continuous variability was performed using two-tailed Student *t* test or a one-way analysis of variance. We performed Pearson chi-square test or Fisher exact test to analyze categorical variability. A ROC curve with an area under the curve (AUC) value was used to evaluate the specificity and sensitivity of the machine learning-based model. Kaplan-Meier (KM) curve analysis and Cox regression analysis with hazard ratio (HR) and 95% confidence interval (CI) were performed to identify the important role of the risk score based on machine learning in clinical prognosis of patients with BCa. Image capturing and the extraction of image features were performed using CellProfiler software (v.3.1.9, Windows). All of these analyses were performed using Statistical Package for Social Sciences 24.0 software (SPSS Inc) and R v.3.6.2 (Windows); a *P*-value < .05 was regarded as significant (Figure 1).

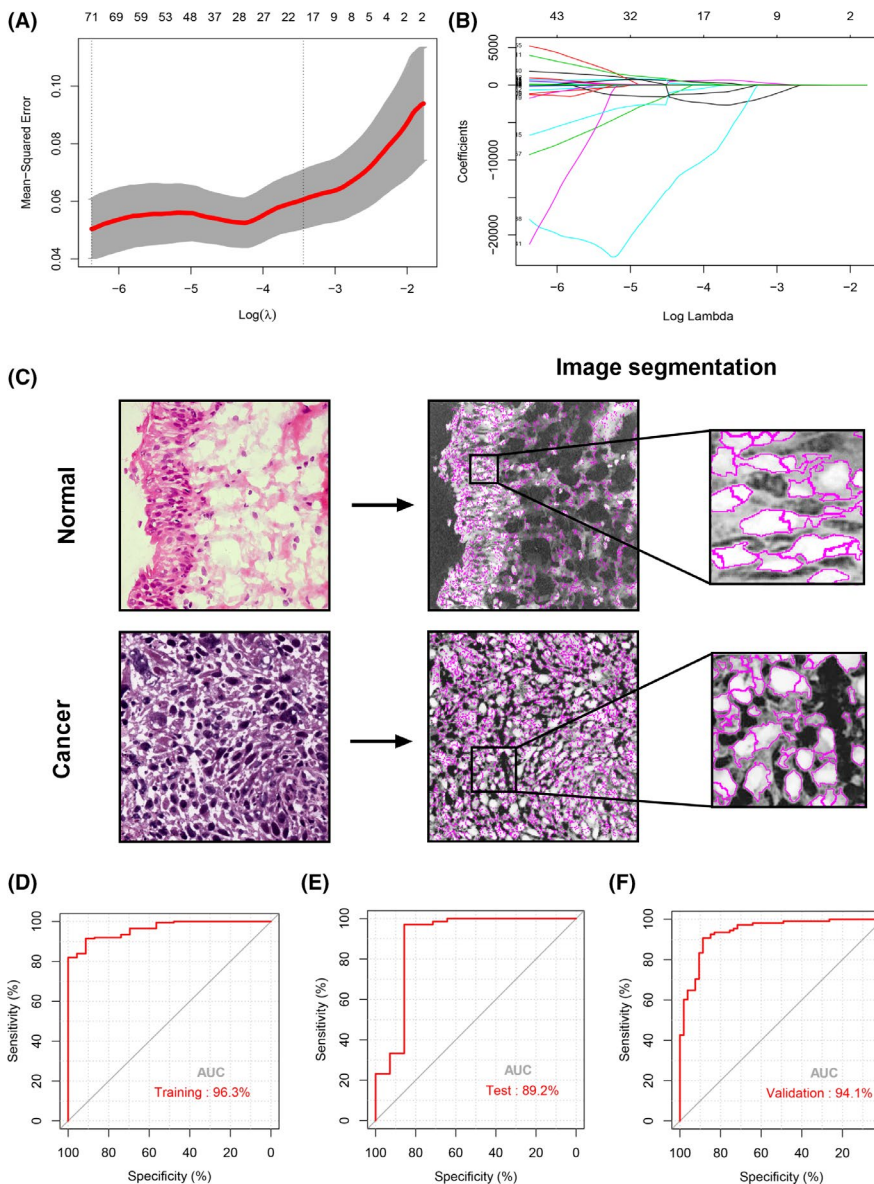


FIGURE 2 Developed and verified the machine learning-based diagnosis model for BCa. A, Ten-fold cross-validated error in LASSO analysis. B, The profile of coefficients in the model at varying levels of penalization plotted against the log (λ) sequence. C, Representative H&E stain and processed images of cancer and normal sample from the training cohort. D-F, The ROC curves of diagnostic score in training cohort, test cohort, and validation cohort, respectively. AUC, area under the curve; BCa, bladder cancer; H&E, hematoxylin-eosin staining; LASSO, least absolute shrinkage and selection operator; ROC, receiver operator characteristics

3 | RESULTS

3.1 | Baseline clinical characteristics of patients with BCa

Baseline characteristics of patients with BCa included in this study are shown in Table S2. Our study had high efficiency in the random division, which showed no significant difference for basic clinical characteristics among training and test cohorts, except for the age composition.

3.2 | High diagnostic efficiency of the machine learning-based diagnosis model for patients with BCa

By using LASSO analysis with 10-fold cross-validation, we identified 22 BCa-related image factors by 10-fold cross-validation (Figure 2A,B). All of the identified image features and their corresponding coefficients are listed in Table S3. As shown in Figure 2C, the automatic segmentation displayed visible differences between BCa tissue and normal bladder tissue. In addition, our machine learning-based diagnosis model performed well in distinguishing BCa samples from normal bladder samples, with AUC values of

96.3%, 89.2% and 94.1% in the training (Figure 2D), test (Figure 2E), and external validation cohorts (Figure 2F), respectively, indicating that the diagnostic model had high diagnostic accuracy.

We next verified the diagnosis model in differential diagnosis of BCa from glandular cystitis. As shown in Figure 3A, notably different identified objects could be found among BCa samples and glandular cystitis samples. The machine learning-based diagnosis model displayed high accuracy in distinguishing patients with BCa from patients with glandular cystitis, with an AUC value of 93.4% in the patient cohort from Shanghai General Hospital. When being compared with non-BCa samples (normal bladder samples and glandular cystitis samples), BCa samples could also be accurately diagnosed through the machine learning-based diagnosis model, with an AUC value of 93.8% (Figure 3C).

3.3 | Important role of machine learning-based risk score for clinical prognosis prediction of patients with BCa

As shown in Figure 4A,B, 18 survival-related image features of BCa samples were identified through LASSO-Cox analysis with 10-fold cross-validation in TCGA cohort, which are also listed in

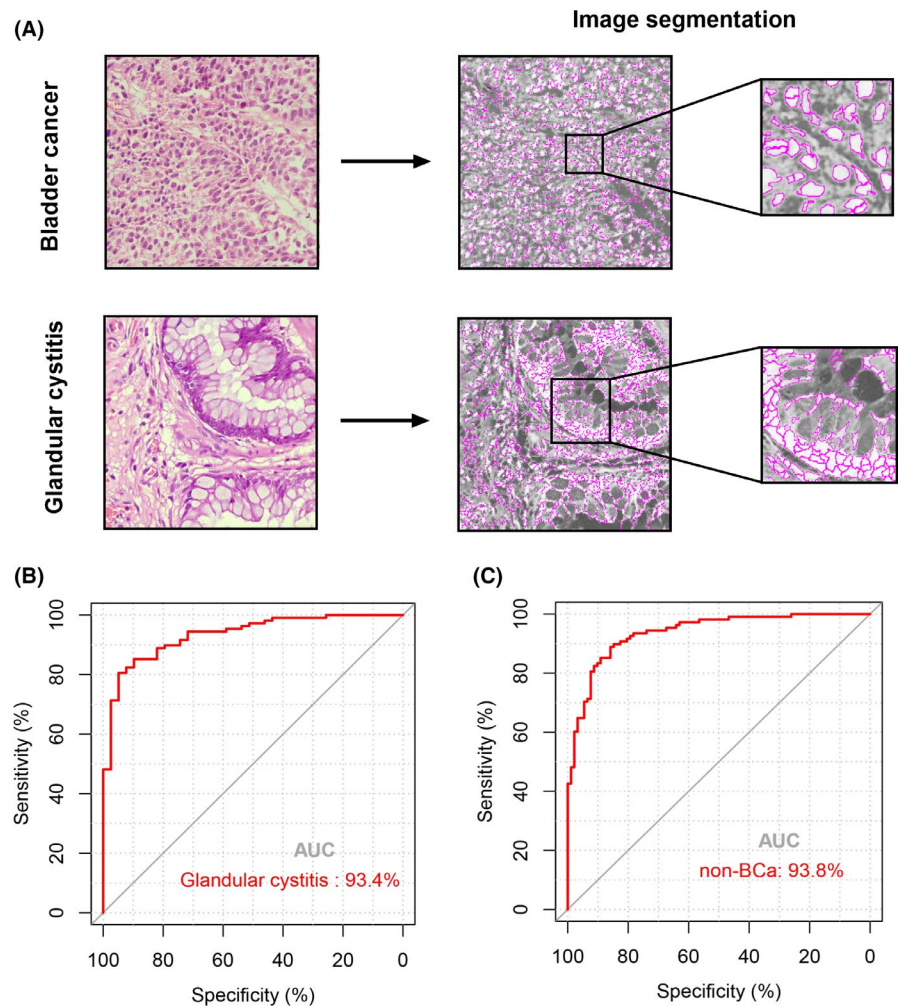


FIGURE 3 Machine learning-based diagnosis model accurately distinguished BCa from glandular cystitis. A, Representative H&E stain and processed images of BCa and glandular cystitis sample from General cohort. B and C, ROC curves for distinguishing BCa from glandular cystitis and non-BCa tissues in General cohort, respectively. AUC, area under the curve; BCa, bladder cancer; H&E, hematoxylin-eosin staining; non-BCa, glandular cystitis and normal tissues; ROC, receiver operator characteristics

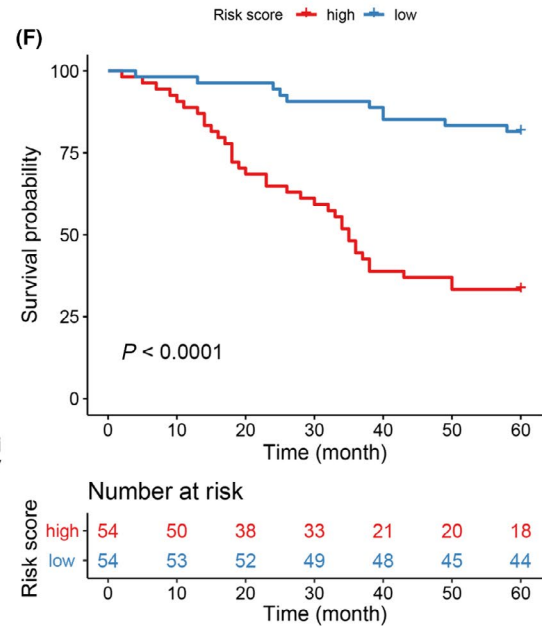
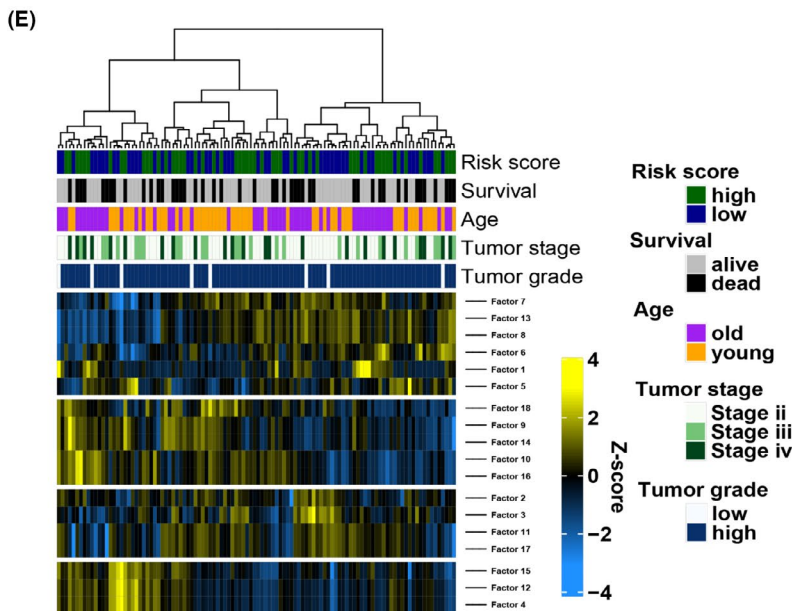
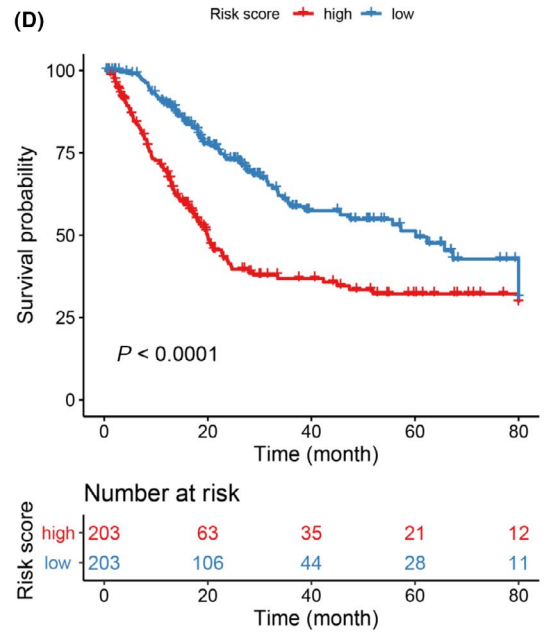
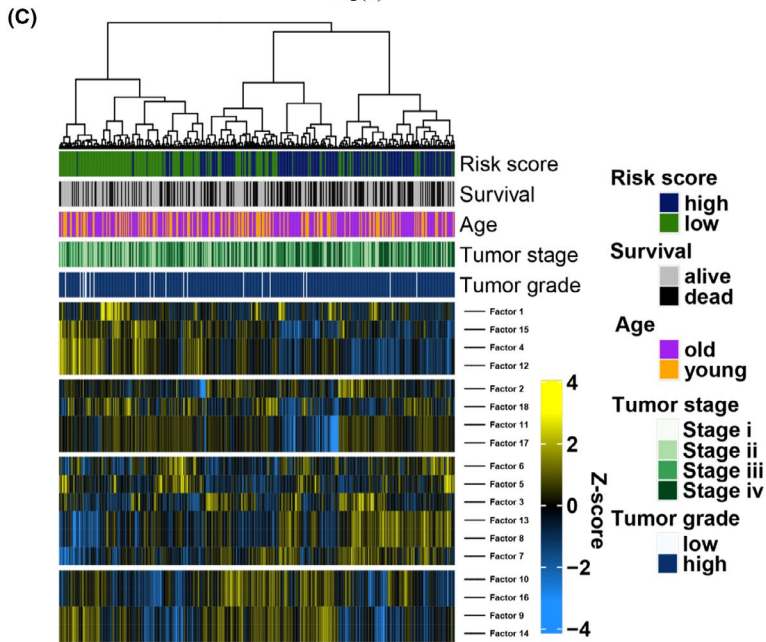
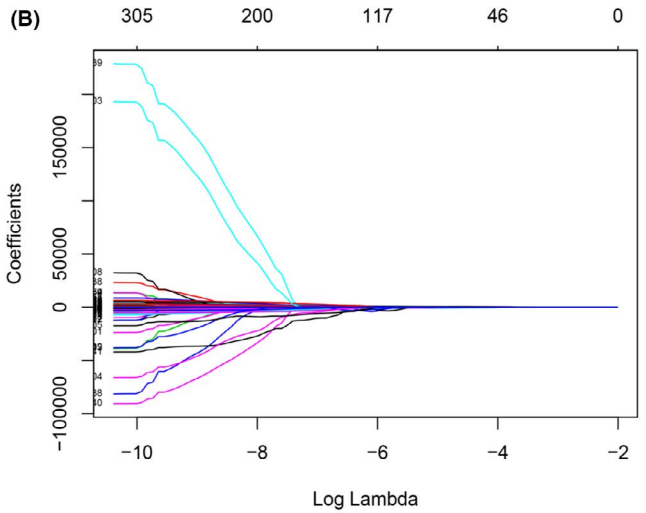
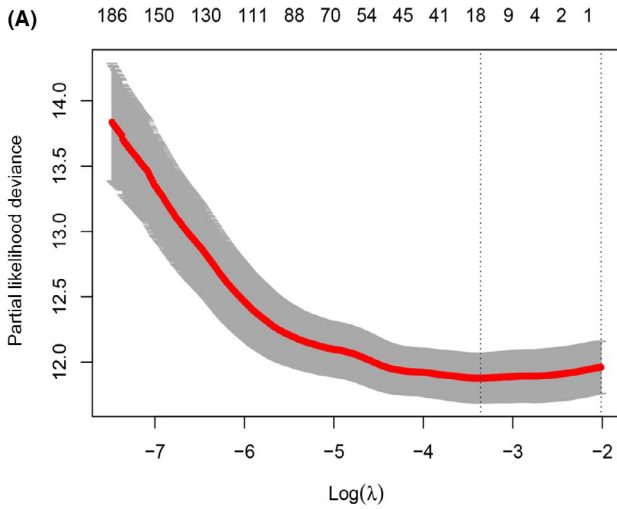


FIGURE 4 Developed and verified the machine learning-based risk score for patients with BCa. A, Ten-fold cross-validated error in LASSO analysis. B, The profile of coefficients in the model at varying levels of penalization plotted against the log (λ) sequence. C and E, Heatmaps demonstrated the distribution of the selected 18 image factors and the risk score by LASSO analysis in training cohort (TCGA cohort) and validation cohort (General cohort), respectively. D and F, Kaplan-Meier survival analysis of overall survival stratified by risk score for patients with BCa from training cohort (TCGA cohort) and validation cohort (General cohort), respectively. The cut-off value of high-risk and low-risk score was defined as the median score of respective cohorts. Feature name of each selected factor was shown in Table S4. BCa, bladder cancer; LASSO, least absolute shrinkage and selection operator; TCGA, The Cancer Genome Atlas

Table S4. The machine learning-based risk score was afterwards analyzed based on the formula presented above. Interestingly, we found that the high-risk score showed significant relevance to high BCa stage and high BCa grade both in TCGA (Figure 4C) and the General cohort (Figure 4E). The overall survival among patients with high-risk or low-risk scores showed significant difference in TCGA cohort (HR = 2.09, 95% CI: 1.56-2.81, $P < .0001$, Figure 4D). We next verified the significant association between risk score and prognosis of BCa in an independent cohort (Figure 4F). Significant difference in overall survival was also found between patients with high-risk and low-risk score in the General cohort (HR = 5.32, 95% CI: 2.95-9.59, $P < .0001$), revealing the important role for machine learning-based risk score for clinical prognosis prediction of patients with BCa.

Further univariate and multivariate Cox regression analyses revealed that our machine learning-based risk score could act as an independent predictor of survival for patients in the TCGA cohort with BCa (Figure 5A), which was also verified in patients from the General cohort with BCa (Figure 5B). Furthermore, significantly higher risk scores were found in patients with BCa with high tumor stages (stage III/IV) (Figure 5C,D). Patients with BCa with high tumor grade were also found to have a higher risk score when compared with patients with low grade tumors (Figure 5E,F).

3.4 | Integration nomogram improves the current survival prediction accuracy for patients with BCa

Current survival prediction for patients with BCa was based on predictable clinical and pathological factors such as clinical tumor stages, pathological tumor grades, and patient ages. To improve current survival prediction accuracy for patients with BCa, an integration nomogram was established based on synthesizing machine learning-based risk score and predictable clinical and pathological factors (Figure 6A). Based on the calibration plot, there was great agreement with practical observations such as 1-, 3-, and 5-year overall survival predictions based on our integration nomogram (Figure 6B). ROC curves for 1-, 3-, and 5-year overall survival predictions revealed that higher prediction accuracy was found in the integration nomogram when compared with clinicopathologic factors (Figure 6C-E). Incremental values of survival prediction accuracy via integration nomograms was also observed in the General cohort (Figure 6F-H), indicating the stable predictive efficacy of the integration nomogram for patients with BCa.

4 | DISCUSSION

Thanks to the rapid development of machine learning algorithms and sophisticated image analysis methods, it appears that high-throughput 'omics, including radiomics, and pathomics, have been gradually used in precision medicine for automatic diagnosis and prognosis prediction.¹³⁻¹⁵ Deep convolutional neural networks could achieve accuracies of 100% and 92% for distinguishing multiple cancer samples and sub-types.¹⁶ For malignant bladder tumors, radiomics-based nomograms could act as a preoperative prediction of lymph node metastasis in bladder carcinoma.¹⁷ MRI-based radiomics nomograms have also been reported to have potential utility for prognosis prediction of patients with BCa.¹⁸

However, due to the indirectness between cancer tissues and radiation images, radiomics might miss important information contained in tumor cells and extracellular matrix. Pathomics digitalizes cancer tissues directly through slide scanning,¹⁹ which might extract histological features to a greater extent.

In this study, we constructed and verified a machine learning-based diagnosis model for patients with BCa based on pathological H&E-stained images of BCa from 2 independent patient cohorts. Our automated diagnostic model could identify BCa when compared with normal bladder tissues with satisfactory AUC values from 89.2% to 96.3%. Furthermore, our diagnosis model could also perform differential diagnosis between BCa and glandular cystitis, with an AUC value of 93.4 in the General cohort.

BCa can be classified into non-muscle invasive bladder cancer (NMIBC) and muscle invasive bladder cancer (MIBC) based on the clinical TNM stages. NMIBC patients showed a decent 5-year overall survival of more than 99%.²⁰ However, despite TNM classifications, morphological patterns could also be associated with the prognosis of patients with BCa. Some poorly differentiated tumors uniformly have extremely poor prognosis regardless of the TNM staging.² Furthermore, BCa at the T2 and T3 stages could be difficult to diagnose on biopsy and transurethral resection samples due to the limitation by the microscope.² Therefore, there is great urgency to develop an effective prognostic prediction method for patients with BCa that is independent of current TNM classification systems.

In this study, by performing machine learning algorithms, we constructed and verified a machine learning-based risk score for clinical prognosis prediction of patients with BCa that could act as an independent predictor of survival for patients with BCa. Patients with high-risk score and low-risk score presented significant overall survival differences among both TCGA and the General cohorts. Additionally, our integration nomogram demonstrated excellent

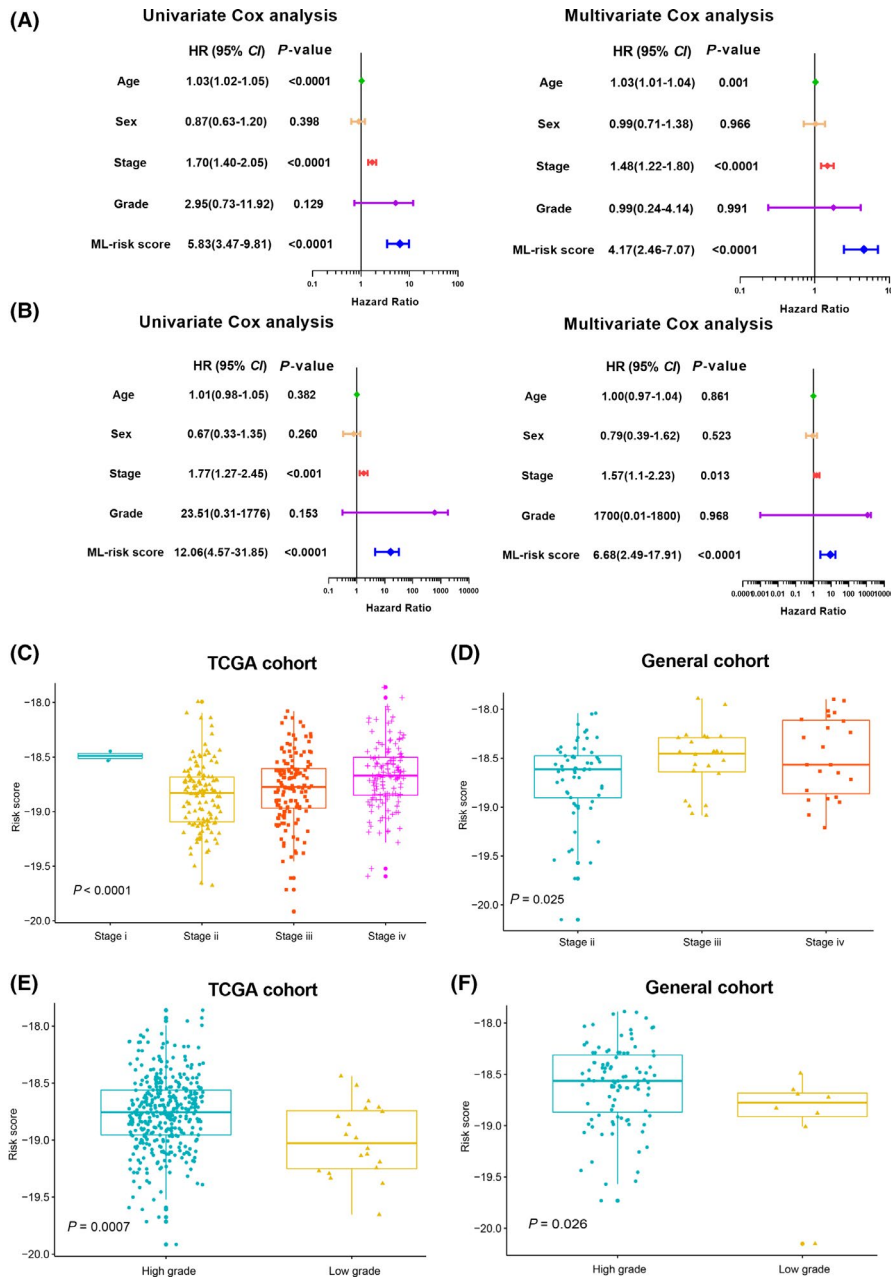


FIGURE 5 Machine learning-based risk score acted as an independent risk factor in overall survival prediction for patients with BCa. A and B, Univariate and multivariate Cox regression analyses of risk score and clinicopathologic features for overall survival of patients with BCa in TCGA cohort and General cohort, respectively. C and D, Significantly higher risk score was found in patients with BCa with high tumor stages in TCGA cohort and General cohort, respectively. E and F, patients with BCa with high tumor grade were found to have higher risk score. BCa, bladder cancer; ML, machine learning; TCGA, The Cancer Genome Atlas

performance in patients with BCa survival prediction. Considering the AUCs, overall survival in 1-, 3-, and 5-y was 77.7%, 83.8% and 81.3%, respectively; our nomogram revealed its great potential in decision-making for various-stage patients with BCa.

Several limitations could also be found in our study. First, less accuracy of our machine learning-based diagnosis model could also be found when comparing with traditional diagnostics by pathologists. Second, the cut-off value of our machine learning-based risk score was defined as the median values in different cohorts, resulting in different ranges of high-risk score between patients from TCGA cohort and the General cohort. Third, our study was retrospective and our machine learning-based BCa diagnostic model needed further

verifications from prospective clinical trials designed in accordance with SPIRIT-AI²¹ and CONSORT-AI.²² However, we innovatively applied pathological image segmentation into clinical practice through our automatic image processing pipeline, and constructed a machine learning-based diagnostic model from a pathomics signature that was easy to understand and use by clinicians without sophisticated computational knowledge. In addition, we presented a novel prognostic indicator for patients with BCa based on a pathomics signature, which differed from conventional clinicopathologic factors.

In conclusion, we constructed and verified machine learning-based pathomics models with functions of automatic BCa diagnosis and survival prediction. Synthesized using conventional clinical and

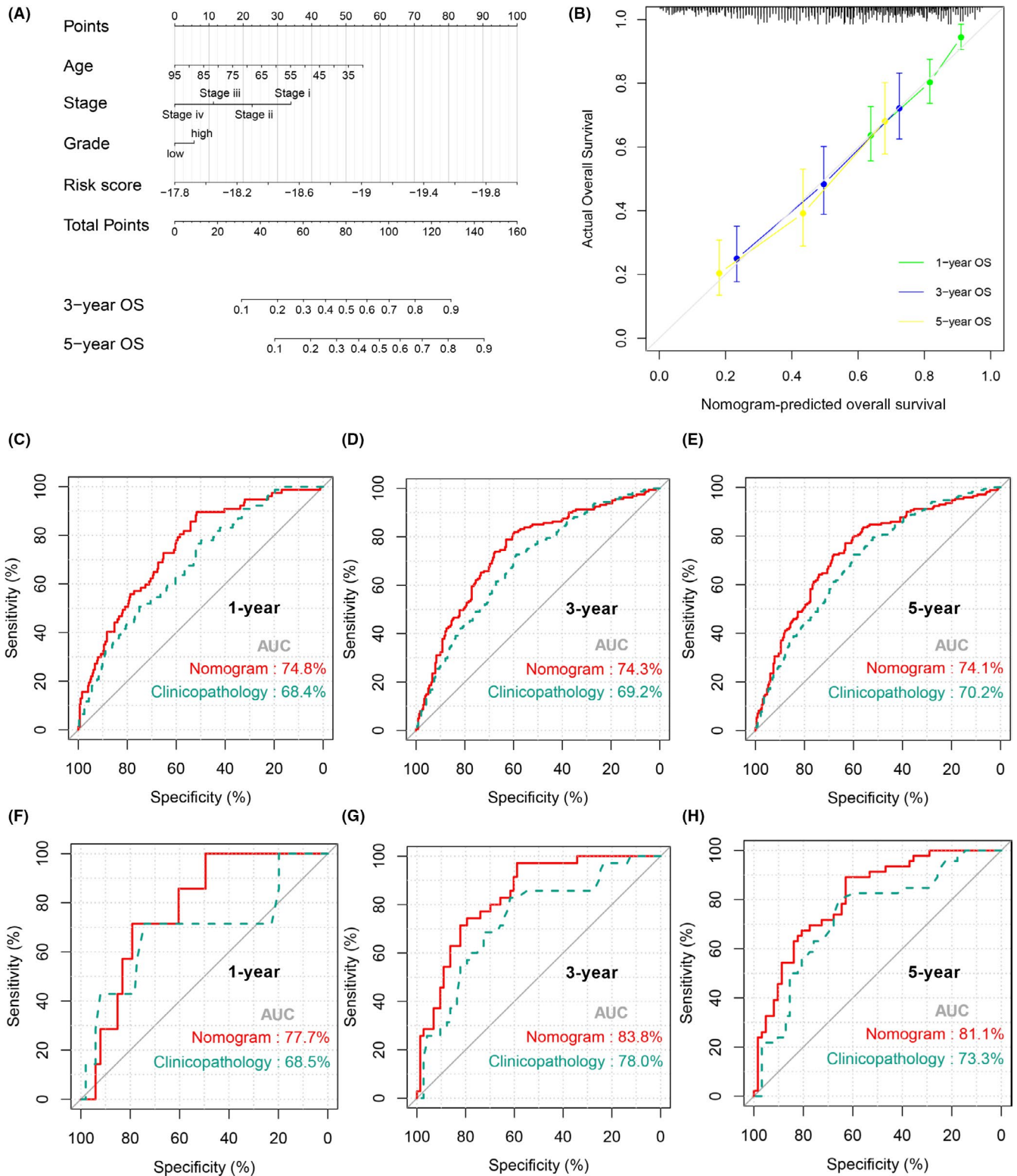


FIGURE 6 Prognostic accuracy of machine learning-based risk score integrated with clinicopathologic factors. A, Nomogram based on risk score and clinicopathologic factors for OS prediction of patients with BCa. B, Evolution of the prognostic nomogram model for 1-, 3-, and 5-y OS prediction. C-E, ROC curves of 1-, 3-, and 5-y OS prediction for the prognostic nomogram model in TCGA cohort. F-H, ROC curves of 1-, 3-, and 5-y OS prediction for the prognostic nomogram model in General cohort. AUC, area under the curve; BCa, bladder cancer; OS, overall survival; ROC, receiver operator characteristics; TCGA, The Cancer Genome Atlas

pathological factors, the machine learning-based risk score was suggested to be an excellent survival predictor for patients with BCa. Nevertheless, prospective studies with large patient cohorts are still needed for further verifications of our pathomics models.

ACKNOWLEDGMENTS

This study was supported by the National Natural Science Foundation of China (81972393 and 81772705).

DISCLOSURE

The authors have no conflict of interest.

ORCID

Xiang Wang  <https://orcid.org/0000-0001-5538-4310>

REFERENCES

- Siegel RL, Miller KD, Jemal A. Cancer statistics, 2020. *CA Cancer J Clin.* 2020;70:7-30.
- Humphrey PA, Moch H, Cubilla AL, et al. The 2016 WHO classification of tumours of the urinary system and male genital organs-part B: prostate and bladder tumours. *Eur Urol.* 2016;70:106-119.
- Lambin P, Rios-Velazquez E, Leijenaar R, et al. Radiomics: extracting more information from medical images using advanced feature analysis. *Eur J Cancer.* 2012;48:441-446.
- Gillies RJ, Kinahan PE, Hricak H. Radiomics: images are more than pictures, they are data. *Radiology.* 2016;278:563-677.
- Ehteshami Bejnordi B, Veta M, Johannes van Diest P, et al. Diagnostic assessment of deep learning algorithms for detection of lymph node metastases in women with breast cancer. *JAMA.* 2017;318:2199-2210.
- Yu K-H, Zhang CE, Berry GJ, et al. Predicting non-small cell lung cancer prognosis by fully automated microscopic pathology image features. *Nat Commun.* 2016;7:12474.
- Kickingereder P, Isensee F, Tursunova I, et al. Automated quantitative tumour response assessment of MRI in neuro-oncology with artificial neural networks: a multicentre, retrospective study. *Lancet Oncol.* 2019;20:728-740.
- Brinker TJ, Hekler A, Enk AH, et al. Deep neural networks are superior to dermatologists in melanoma image classification. *Eur J Cancer.* 2019;119:11-17.
- Carpenter AE, Jones TR, Lamprecht MR, et al. Cell Profiler: image analysis software for identifying and quantifying cell phenotypes. *Genome Biol.* 2006;7:R100.
- Kamentsky L, Jones TR, Fraser A, et al. Improved structure, function and compatibility for cell profiler: modular high-throughput image analysis software. *Bioinformatics.* 2011;27:1179-1180.
- Friedman J, Hastie T, Tibshirani R. Regularization paths for generalized linear models via coordinate descent. *J Stat Softw.* 2010;33:1-22.
- Simon N, Friedman J, Hastie T, et al. Regularization paths for Cox's proportional hazards model via coordinate descent. *J Stat Softw.* 2011;39:1-13.
- Lambin P, Leijenaar RTH, Deist TM, et al. Radiomics: the bridge between medical imaging and personalized medicine. *Nat Rev Clin Oncol.* 2017;14:749-762.
- Cao R, Yang F, Ma S-C, et al. Development and interpretation of a pathomics-based model for the prediction of microsatellite instability in Colorectal Cancer. *Theranostics.* 2020;10:11080-11091.
- Jiang Y, Jin C, Yu H, et al. Development and validation of a deep learning CT signature to predict survival and chemotherapy benefit in gastric cancer: a multicenter, retrospective study. *Ann Surg.* 2020. <https://doi.org/10.1097/SLA.0000000000003778>. Online ahead of print
- Khosravi P, Kazemi E, Imielinski M, et al. Deep convolutional neural networks enable discrimination of heterogeneous digital pathology images. *EBioMedicine.* 2018;27:317-328.
- Wu S, Zheng J, Li Y, et al. A radiomics nomogram for the preoperative prediction of lymph node metastasis in bladder cancer. *Clin Cancer Res.* 2017;23:6904-6911.
- Wu S, Zheng J, Li Y, et al. Development and validation of an MRI-based radiomics signature for the preoperative prediction of lymph node metastasis in bladder cancer. *EBioMedicine.* 2018;34:76-84.
- Madabhushi A, Lee G. Image analysis and machine learning in digital pathology: challenges and opportunities. *Med Image Anal.* 2016;33:170-175.
- Flaig TW, Spiess PE, Agarwal N, et al. NCCN guidelines insights: bladder cancer, version 5.2018. *J Natl Compr Canc Netw.* 2018;16:1041-1053.
- Cruz Rivera S, Liu X, Chan A-W, et al. Guidelines for clinical trial protocols for interventions involving artificial intelligence: the SPIRIT-AI extension. *Nat Med.* 2020;26:1351-1363.
- Liu X, Cruz Rivera S, Moher D, et al. Reporting guidelines for clinical trial reports for interventions involving artificial intelligence: the CONSORT-AI extension. *Nat Med.* 2020;26:1364-1374.

SUPPORTING INFORMATION

Additional supporting information may be found online in the Supporting Information section.

How to cite this article: Chen S, Jiang L, Zheng X, et al. Clinical use of machine learning-based pathomics signature for diagnosis and survival prediction of bladder cancer. *Cancer Sci.* 2021;112:2905-2914. <https://doi.org/10.1111/cas.14927>